

TIME OF FLIGHT (TOF) MODE OF OPERATION IN IONOSPHERIC ION DRIFT MEASUREMENTS

Bankov L.G., Vassileva A.K.

Space Research Institute – Bulgarian Academy of Sciences

Abstract

During the past 30 years, ion drift measurements were a very powerful way to study the Earth's ionosphere dynamics in the context of the Sun-Earth relation processes. Here, we propose a combined use of Time-Of-Flight reflectron as a part of the modified Ion Drift Meter (IDM) sensor to obtain valuable mass-spectra and ram ion speed in parallel to the IDM transverse ion drift velocity measurements. This in fact could reduce the measuring technique to a single-sensor IDM/TOF mass-spectrometer.

INTRODUCTION

In situ ion drift measurements in the Earth's ionosphere by means of ion probes onboard the satellites, proceed under the basic assumption that ion thermal speed is small enough in comparison to the satellite velocity, which is almost well satisfied within the entire F-region. S.P. Korolev was the first to propose ion sensors as a part of the ballistic missile angular orientation system in earlier 60's [1]. This measuring technique appeared to be sensitive to the ionospheric ion drift motion, which causes a spurious output signal to the orientation system. Ion drift measurements were proposed as an input current balance method of a double planar ion probe mounted away from the satellite velocity vector on the COSMOS-184 satellite [2]. An improved techniques by means of a Retarding Potential Analyzer (RPA) and IDM for ram and transverse ion drift measurements was used on the Atmosphere Explorer C,D,E satellites [3]. It was shown by the authors that ram drift component could be calculated after a fitting procedure of the current-to-voltage curve from the RPA sensor if additional mass-spectrometer information about the present ion species is available. Also, the current ratio offset from the opposite collector pairs of the IDM sensor is proportional to the value of the transverse yaw (horizontal) and

pitch (vertical) ion drift velocity components. Later, this method was successfully used on the Dynamics Explorer-B, San Marco, DMSP, ROCSAT etc. satellites. On the Intercosmos "Bulgaria-1300" (ICB-1300) satellite IDM/RPA sensors for ion drift velocity measurements were similarly used at heights of 800km to 1000km [4]. At these heights, the ICB-1300 satellite passed almost beneath, through or higher than O^+/H^+ transition level. In result, the evaluation of the ram velocity from the RPA current-to-voltage curve becomes difficult in the presence of only two major species (predominant O^+ ions at daylight and H^+/He^+ ions at night) without relevant mass-spectrometric data. For the same reason, the IDM output was affected by the presence of light ions at around midnight local times [5]. During an active experiment mission on the Intercosmos 24-"ACTIVE" satellite, a modified IDM sensor with five collector segments as RPA (central collector) and IDM (two side collector pairs) for simultaneous measurement of both components were used [6]. Fast wide dynamic range measurements of ion drift by Digital Ion Drift Meter (DIDM) on the CHAMP satellite were made [7]. The DIDM consists of a pin hole camera type of sensors with 2D view of input ion flow projection on position-sensitive micro-channel plate (MCP) detector for determination of X/Y shift of count rate maximum due to the presence of ionospheric ion drift component. The sensitivity and accuracy of the method depend on the exact determination of the main count rate maximum position observed on the 2D camera view. At present, it is commonly accepted to use RPA for ram drift component and the IDM for transverse velocity components because of their high accuracy and sufficient sensitivity. One of the important uncertainties of this measuring technique is addressed to the time/space discrepancy between the time resolution of RPA and IDM, accordingly. Yaw and pitch ion drift velocities could be measured with relatively high temporal resolution with IDM instrument limited only by the level of the input current flow. Ram ion drift velocity could be calculated from RPA current-to-voltage curves taken only a few times per second because of the limitation of narrow bandwidth and accuracy at low input current levels when high retarding voltage is applied. Here, we propose a combination of an IDM sensor used on the IC-24 satellite [6] with a TOF mass-reflectron as a mass-spectra/ion drift sensor with relatively high time/space resolution for both ram and transverse ion drift velocity components. The central collector of the IDM [6] could be also used as a duct sensor for ion density irregularities observation and in-flight calibration with the same time resolution. The expected advantages of the proposed method could be summarized as follows:

- Fast mass-spectrometry of the ionospheric ions with high mass resolution
- Direct estimation of ram ion drift velocity and satellite skin potential
- Fast ion drift measurement of both ram and transverse velocity components
- High resolution measurements of ion density irregularities for different ion species

TOF mass-reflectron is a well-known instrument for laboratory laser mass-spectrometry applications with impulsive ion source. Its simple construction and relatively good mass resolution make it quite convenient for satellite application [8,9].

BASIC PRINCIPLES OF THE METHOD

In the Earth's ionosphere, at the height above the bottom side F-region, where ion-neutral collision frequency becomes small enough compared to ion gyro frequency, ions and electrons drift together perpendicularly to the external electric field \mathbf{E} and the Earth's magnetic field \mathbf{B} with drift velocity: $\mathbf{V}_d = \mathbf{E} \times \mathbf{B} / B^2$

Following [3], in a frame of reference moving with the satellite's velocity \mathbf{V}_{sat} , the main task to measure \mathbf{V}_d could be divided in two stages, measuring separately the perpendicular ($\mathbf{V}_{d\perp}$) and ram ($\mathbf{V}_{d\parallel}$) components in respect to \mathbf{V}_{sat} . While the measuring technique of $\mathbf{V}_{d\perp}$ is fully described in [3], here we will present a more detailed view on the proposed time-of-flight method of ram ion drift $\mathbf{V}_{d\parallel}$ measurements. If we assume satellite skin potential $U_{sat} = 0\text{V}$, in a satellite frame of reference ionospheric ions have a ram kinetic energy $E_i = m_i (\mathbf{V}_{sat} + \mathbf{V}_{d\parallel})^2 / 2$ where m_i is the ion mass of the different ion species. We assume ram drift velocity equal for different ion species which means pure electrodynamic drift motion. Let us consider the main steps from RPA toward TOF measurement of the $\mathbf{V}_{d\parallel}$. Fig.1(a) shows an example of the expected current-to-voltage curve of a classic RPA sensor for H^+ , He^+ , O^+ and NO^+ ions (other ion species are omitted for simplicity). The C-V curve is an integral characteristic of the different ion energy distribution functions in the satellite frame of reference. The positive ram velocity $\mathbf{V}_{d\parallel}$ augments the energy of every ion species to the higher energies and vice versa, the negative $\mathbf{V}_{d\parallel}$ reduces ion energy of every ion species in a proportional to m_i way. The satellite skin potential U_{sat} shifts the entire C-V

curve in the energy frame of reference, not changing the relative distance between mass peaks. The corresponding plasma parameters could be found by means of the least square technique used to fit the C-V curve of RPA for ion density N_i , ion mass m_i , ion temperature T_i , ram ion drift $V_{d\parallel}$ and satellite potential U_{sat} . An accurate solution of this task could be obtained with the support of mass-spectrometer data for the density of the present ion species [3]. On panel (b) of Fig.1, we show a sketch of ion energy distribution functions already shown on panel (a) in corresponding gray scale amplitudes against the relative thermal velocity distribution function for each ion species around $V_i = (V_{sat} + V_{d\parallel})$ under the assumption $U_{sat} = 0v$ (Y- axis on the right-hand side of the panel). At a given ion temperature T_i , ion thermal velocity V_{th} is larger for light ions, decreasing by a factor of $1/\sqrt{m_i}$ to the higher mass numbers, as illustrated on the right-hand side of the panel for equal density H^+ , He^+ , O^+ and NO^+ ions. Obviously, in this case TOF mass separation could not be used when different ions enter the sensor with equal ram velocity V_i . In the same format, panel (c) of Fig.1 shows the changes in velocity distribution for different ion species in case of negative ($U_{sat} < 0v$) satellite skin potential and an acceleration with short negative impulse U_{ac} is used. The relative energy shift of the peak in thermal velocity distribution functions is proportional to the ion mass number as $\sqrt{(2e(U_{ac}+U_{sat})/m_i)}$ where e-units charge. Ion speed decreases with ion mass as $1/\sqrt{m_i}$ for a given $U=U_{sat}+U_{ac}$. The TOF mass spectrum after impulse acceleration is shown on the right-hand side of the panel for the expected mass resolution limited by the thermal spread of the different ion species. Better results could be obtained with higher negative amplitude of U, but this will decrease significantly flight time for the ions at fixed distance. The accurate estimation of the U_{ac} amplitude and optimal flight distance gives provides an opportunity for mass separation with moderate mass resolution. Mass resolution at low-mass numbers is very sensitive to the value of accelerating potential U. At least two ion species presented in the mass-spectrum should be available to calculate U and V_i . The main problem is to evaluate the exact position of the mass peak for low ion mass numbers because of the large thermal velocity spread occurring in this part of the spectrum. The shape of the peaks depends on the flight time spread around the central value t_j , which corresponds to the ion velocity thermal spread ($j = 1, n$ number of observed mass peaks). Considerably better mass resolution could be achieved by time and/or space focusing of the ions. As it was mentioned above, we suggest linear TOF mass reflectron to be used as mass-spectrometer section with relatively good mass-resolution for accurate mass peak position observation. Fig. 1(d) represents the expected changes in

mass resolution when the TOF mass-reflectron is used for flight time focusing of the different ions accelerated with the negative U_{ac} impulse at

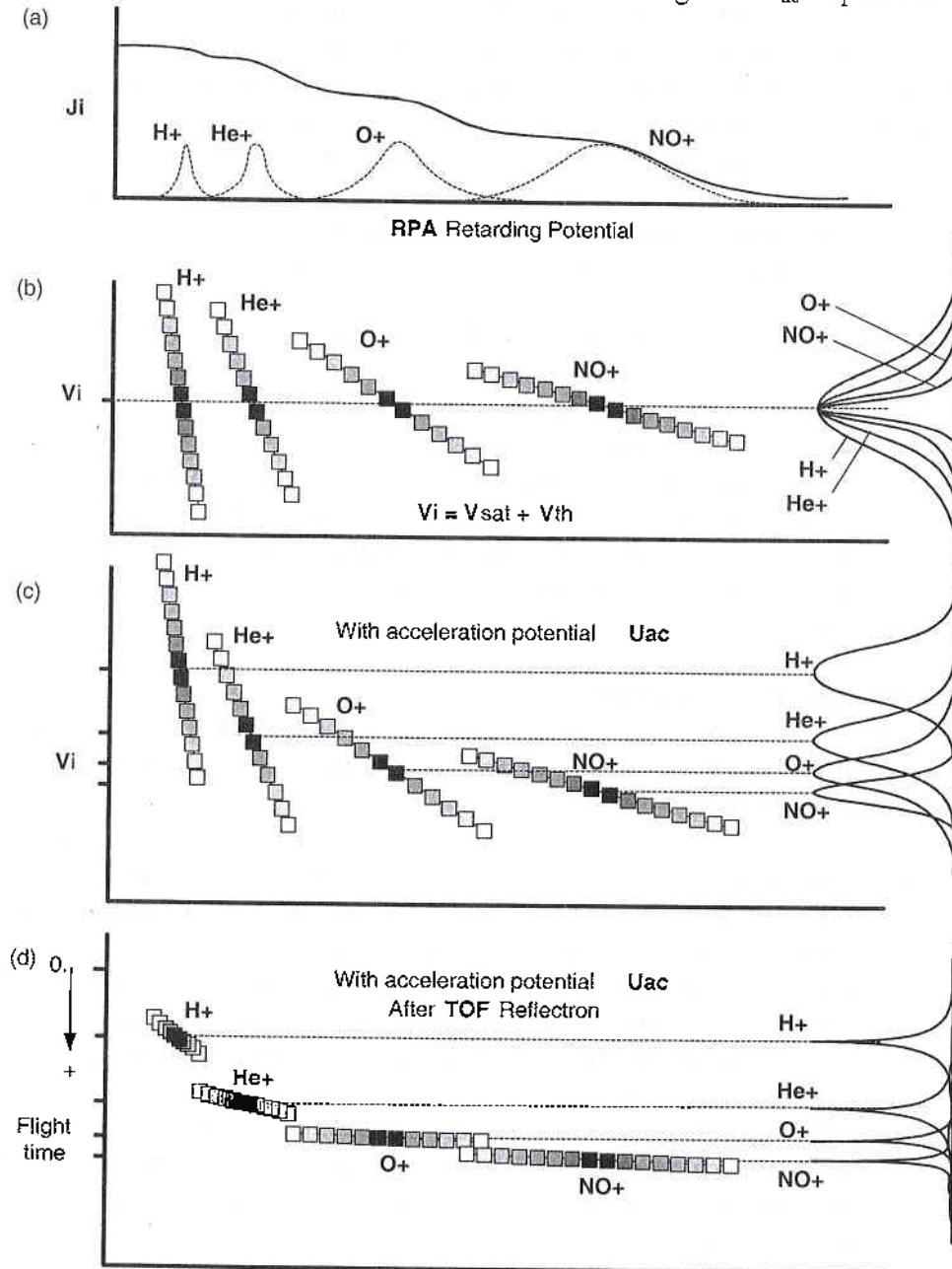


Fig.1

the moment t_0 . The left-hand side Y-axis of the panel shows the relative flight time for different ions after t_0 . Mass peaks become narrow, because of the used time compensation for different ions inside the reflectron flight space (faster ions with equal mass fly at longer distances than slower ones) [8]. Ram ion drift $V_{d\parallel}$ shifts mass peaks toward shorter ($V_{d\parallel} > 0$) or larger ($V_{d\parallel} < 0$) flight times. The changes in satellite skin potential ($U_{sat} < 0$) affect the relative distance between the peaks while added ion speed becomes proportional to $\sqrt{(2e(U_{ac} + U_{sat})/m_i)}$. To obtain V_i and U , let us consider that two ion species are observed in the mass spectrum. If we assume L to be the ions flight distance we can write for the two observed ion species:

$$(1) \quad (L/t_1)^2 = V_i^2 + 2eU/m_{i1} \quad (L/t_2)^2 = V_i^2 + 2eU/m_{i2}$$

These equations (1) could be solved together for $V_i = (V_{sat} + V_{d\parallel})$ and $U = (U_{sat} + U_{ac})$. With accurate attitude information for V_{sat} and amplitude of U_{ac} a correct value for $V_{d\parallel}$ and U_{sat} could be found. More than two registered ion mass peaks will increase the accuracy of measurement. In conclusion, if we neglect T_i measurements, TOF reflectron mass-spectrometry could be an effective method for ram drift velocity measurements.

INSTRUMENTATION

The space application of the measuring technique of TOF/IDM mass reflectron proposed here could be achieved as flight instrument limited by the following factors:

- Input ion flow $N_i \cdot V_{sat}$ at ionospheric heights varies approximately from $10^8 - 10^{12}$ (particles $\cdot s^{-1} \cdot cm^{-2}$) for $10^2 - 10^6$ cm^{-3} of ambient ion density. Input modulation of this flow reduces it from 10^1 to 10^5 possible counts during mass spectrum registration. In addition, the transparency of the whole system and the effectiveness of the MCP registration could reduce this count rate by a factor of about 10-50.
- A maximum count rate for the MCP registration module of up to 10^8 counts/s becomes the absolute upper limit of about $5 \cdot 10^3$ counts per mass-spectrum, if the mechanical and electrical parameters of the TOF section refer to a $50 \mu s$ maximum flight time. It is more realistic to assume $1 - 2 \cdot 10^3$.
- The direct solar UV irradiance and the high-energy particles impact cause background noise in the MCP module. High quality optical trap for UV and shielded MCP module have to be used.

The combined influence of these factors decreases the threshold level sensitivity for single mass-spectrum registration. To expand the dynamical characteristics of the instrument, an accumulation of the counts for repetitive mass-spectra registration and/or a parallel current mode for MCP could be used.

A sketch of the possible solution for mechanical design of the sensor is shown in Fig.2. As it can be seen from the side view of the instrument, the X-axis is aligned along the satellite velocity vector V_{sat} . On the upper part of level **A-A**, the schematic configuration of the IDM sensor with five collector segments is shown. A square input aperture is used to collimate input ion flow before reaching the collector's surface. Grounded grids G_1 and G_2 provide field-free drift space inside the IDM sensor. The input ion flow enters drift space with an angular offset from the X-axis due to the transverse ion drift component. In result, measured current ratio from opposite collector pairs C_1/C_3 is a proportional production of the arrival angle of input ion flow in the X-Y plane (C_2 and C_4 are not seen). Grid G_3 could be grounded or slightly positive to prevent the light ions from reaching the collectors in the special IDM mode [5]. Suppressor grid G_4 has constant negative potential to minimize the photoemission current from the collector surface. A central collector C_5 with adjacent segments could be used for fast total ion current measurements and absolute in-flight calibration of the TOF mass-spectrometer [6]. In the middle of the C_5 , along the X-axis, an axial input hole for the TOF section is made. Now let us consider the TOF section operation. A small part of the input ion flow enters the TOF section through input modulator G_5 . The TOF section consists of two major stages: free field (G_6, G_7) drift space with length L and reflectron section with length d . G_8 grid is under positive potential U_r . Chevron type dual micro channel plates with a central hole are used for incident ion detection. The TOF section is continuously connected to a negative potential U_m where $U_m \ll U_{ac}$ (fig.3), while modulator G_5 is continuously under U_{ac} potential. If we assume $U_{ac} = -10v$ the single mass spectrum duration is about $50\mu s$ if $L+d$ is about $0.25m$.

At moment t_0 , the ions enter G_5 volume, accelerated with energy of $10eV$ in addition to their ram energy in the satellite frame of reference [fig.3]. After some time t_{mod} to the end of mass registration, we close switch SW1 of G_5 modulator to U_m and the rest of incoming ions will be accelerated to energy of about eU_m . During this time, a portion of ions from the internal volume of the modulator will enter the TOF section, accelerated only to the energy of $10eV$. Within the next $50\mu s$ the TOF ion mass

spectrum of this portion is registered on MCP. If we accept having 100 registered points on the spectrum, a 500ns count window for MCP has to be used. To minimize time spread of input ion impulse within the registration period of 50 μ s, the TOF section potential is settled to $U_m \ll U_{ac}$. During ion mass spectra registration of the input ion pulse with $E_i=10$ ev, ions entering the TOF section will be accelerated to energy $E_{im}=eU_m$. These particles fly through the TOF section with energy sufficient enough to overcome the positive potential U_r applied to G_8 ($E_{im} \gg eU_r$). This type of modulation permits us to have in less than 100ns, ion pulses available for TOF mass-spectrometry. In parallel, registration of mass spectra in current mode of operation for an MCP with fast ADC registration boosts the actual output dynamics and sensitivity of the method. Similar modulation technique has been used for the energy-mass analyser KSANI on the IC-24 satellite [6]. To prevent the influence of incident solar ultraviolet radiation, UV light traps have to be used to minimize scattered UV before reaching the MCP module. Suppressor grid G_9 with small negative potential prevents the photoemission electrons emitted from the light trap section to reach the MCP sensor. Single ion mass TOF spectra registration could be repeated an appropriate number of times to optimize threshold sensitivity level. An adaptive algorithm to input ion flow parameters could be used to provide for flexible characteristics of the instrument and onboard data processing.

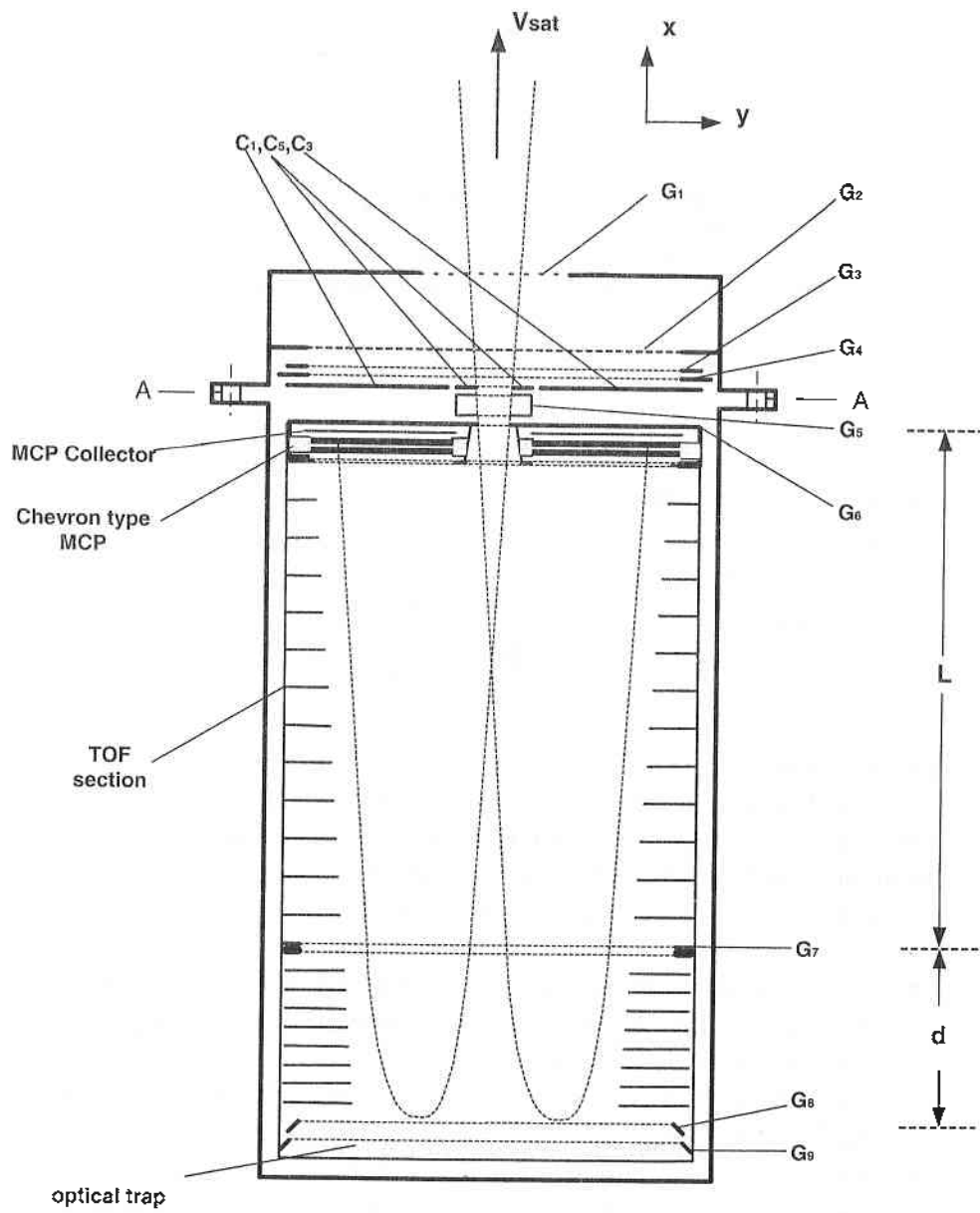


Fig.2

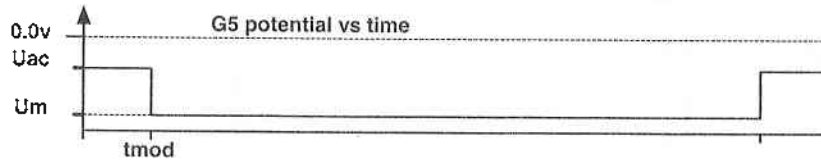
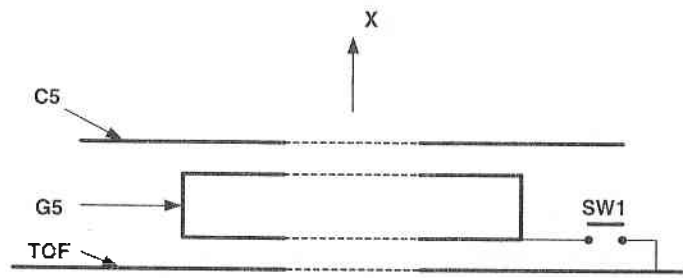


Fig.3

CONCLUSION

The most important reason to evaluate the IDM/TOF measuring technique proposed here is to combine high-speed IDM transverse ion drift measurement with the high-speed performance of Time-of-Flight mass-spectrometry. The main objectives could be as follows:

- With an appropriate operation mode for TOF section it is possible to provide $1 \div 10$ ms ($20 \div 200$ shots) measuring time for a single mass-spectrum same as IDM opportunities
- The simplicity of equations (1) suppose onboard processing of the m_i , $V_{d\parallel}$ and U_{sat}
- The MCP sensor with centered hole combined with mass-reflectron section provides a good opportunity to prevent incident ions or UV radiation from reaching the registration module
- Continuous measurements of ion density irregularities by IDM could be successfully used for in-flight calibration of the mass-spectrometer

References

1. S.P. Korolev activity in documents, Moscow, Nauka, 1980
2. Y.I.Galperin et al., Direct measurements of ion drift velocity in the upper atmosphere during a magnetic storm, *Kosm.Issl.*, 11, 273, 1973.
3. W.B.Hanson and R.A.Heelis, Technics for measuring bulk gas motion from satellites, *Space Sci. Instrum.*, 1, 493, 1975.
4. L.G.Bankov et al., An instrument for total ion drift velocity measurements aboard the Intercosmos Bulgaria-1300 satellite, *Adv. Space Res.*, 2, 71, 1983.
5. L.G. Bankov et al., A study of the retarding potential influence on transverse ion drift velocity measurements by means of ion drift meter onboard ICB-1300 satellite,
6. L.G.Bankov et al., Critical ionization velocity CIV experiment XANI onboard the Intercosmos 24-ACTIVE satellite, *Adv.Space Res.*, 13, 10, 193, 1996.
7. D.L.Cookel and C.J.Roth, The digital ion drift meter on CHAMP, status, calibration and data, 3M41C, 2002 AGU Spring meeting.
8. B.A.Mamirin and D.V.Shmik, Linear mass-reflectron, *JETPhys.*, 5, 76, 1500, 1979.
9. Managadze N.G. et al., Quantitative analysis of metal alloys, ceramics, minerals without standard samples with help of compact laser TOF mass-spectrometer, 45 Conference of ASMS, Palm Springs, USA, 1997.

ИЗМЕРВАНЕ НА ЙОННИЯ ДРЕЙФ В ЙОНОСФЕРАТА С ИЗПОЛЗВАНЕ НА РЕЖИМ ВРЕМЕ ЗА ПРЕЛИТАНЕ

Л.Банков и А.Василева

Резюме

През последните 30 години измерванията на йонния дрейф бяха много мощен начин за изучаване на динамиката на земната йоносфера в контекста на процесите на слънчево-земните взаимодействия. В настоящата работа ние предлагаме комбинирано използване на електростатичен рефлектрон с време за прелитане (Time Of Flight-TOF), като част от модифициран йонен дрейфметър (Ion Drift Meter - IDM) за едновременно определяне както на паралелната така и на напречната скорост на йонния дрейф. Това на практика би могло да сведе измервателната методика до използването на един общ датчик TOF/IDM.